Hindawi Publishing Corporation
Advances in Meteorology
Volume 2014, Article ID 179301, 10 pages
http://dx.doi.org/10.1155/2014/179301

Research Article

Black Carbon and Elemental Carbon from Postharvest Agricultural-Waste Burning Emissions in the Indo-Gangetic Plain

Atinderpal Singh,[1] Prashant Rajput,[2] Deepti Sharma,[1] M. M. Sarin,[2] and Darshan Singh[1]

[1] *Department of Physics, Punjabi University, Patiala 147 002, India*
[2] *Geosciences Division, Physical Research Laboratory, Ahmedabad 380 009, India*

Correspondence should be addressed to Darshan Singh; dsjphy@yahoo.com

Received 21 March 2013; Revised 10 June 2013; Accepted 8 January 2014; Published 26 February 2014

Academic Editor: Lucas Alados-Arboledas

We compare the mass concentrations of black carbon (BC) and elemental carbon (EC) from different emissions in the Indo-Gangetic Plain (IGP), using optical (Aethalometer; 880 nm) and thermooptical technique (EC-OC analyzer; 678 nm), respectively. The fractional contribution of BC mass concentration measured at two different channels (370 and 880 nm), OC/EC ratio, and non-sea-salt K^+/EC ratios have been systematically monitored for representing the source characteristics of BC and EC in this study. The mass concentrations of BC varied from 8.5 to 19.6, 2.4 to 18.2, and 2.2 to 9.4 $\mu g\,m^{-3}$ during October-November (paddy-residue burning emission), December–March (emission from bio- and fossil-fuel combustion) and April-May (wheat-residue burning emission), respectively. In contrast, the mass concentrations of EC varied from 3.8 to 17.5, 2.3 to 8.9, and 2.0 to 8.8 $\mu g\,m^{-3}$ during these emissions, respectively. The BC/EC ratios conspicuously greater than 1.0 have been observed during paddy-residue burning emissions associated with high mass concentrations of EC, OC, and OC/EC ratio. The Ångström exponent (α) derived from Aethalometer data is approximately 1.5 for the postharvest agricultural-waste burning emissions, hitherto unknown for the IGP. The mass absorption efficiency (MAE) of BC and EC centers at ~1–4 $m^2\,g^{-1}$ and 2-3 $m^2\,g^{-1}$ during the entire study period in the IGP.

1. Introduction

Black carbon (BC) and elemental carbon (EC) are primary constituents of atmospheric aerosols produced from incomplete combustion of fossil fuel vis-à-vis biomass burning emission [1]. The atmospheric significance of BC and EC is due to their potential light absorption characteristics and recognition as a driver of the global warming demands for their spatial distribution and temporal variability records [2, 3]. Furthermore, the assessment of global climate change also reports a large uncertainty in the estimation of aerosol radiative forcing, arising mainly due to complexity in absorbing and scattering particles characteristics [4]. In addition, the impact of these light-absorbing aerosols on Indian summer monsoon and heating rates of the elevated regions of the Himalayan-Tibetan plateau has been realized [5, 6]. Thus, the records on atmospheric variability of BC as well as EC are significantly important for assessing its impact on climate. A couple of earlier studies suggest the assessment of the role of organic aerosols when assessing the impact of absorbing aerosols (BC, EC) on the radiative forcing estimations [2, 7]. To assess the characteristics of BC and EC from various kinds of biomass burning emissions, we have conducted a campaign from a source region in the Indo-Gangetic Plain (IGP).

The terminology of black carbon and elemental carbon (BC, EC) has originated from their measurement technique. The BC refers to the light-absorbing part of the carbonaceous aerosols and is determined using optical method. In contrast, the EC is a refractory constituent of the aerosols and is determined using thermooptical technique under oxidizing condition. In this study, we also adhere to this conventional terminology and report that BC concentrations are measured optically by Aethalometer at 880 nm, whereas EC concentrations are measured using thermooptical method on

EC-OC analyzer at 678 nm. The optical method monitors the attenuation of light through aerosol-loaded filter at a given wavelength (here 880 nm by Aethalometer) and uses a constant attenuation cross section (σ_{ATN}) of 16.6 m^2 g^{-1} to determine the BC mass concentrations. However, several studies have addressed the issue on the spatial variability of σ_{ATN} [8–11]. In contrast, the thermooptical method (EC-OC analyzer at 678 nm) determines the mass concentrations of organic and elemental carbon (OC, EC) in aerosols based on their chemical properties [10, 11].

The main objective of this study is to assess the characteristics of elemental and black carbon (EC and BC) based on their mass absorption efficiency (MAE). The fractional contribution of BC at 370 nm and 880 nm exhibits a typical signature of biomass burning emission during the paddy- and wheat-residue burning. In contrast, during wintertime the BC from mixed sources (fossil-fuel combustion and biomass burning) is observed. A similar characteristic for EC is also observed based on the chemical tracers such as the OC/EC and nss-K^+/EC ratios (non-sea-salt: nss-K^+). Our study shows that BC/EC ratios are conspicuously greater than 1 during the postharvest paddy-residue burning emission (associated with relatively high concentration of EC, OC, and OC/EC ratio). Furthermore, we document the Ångström exponent (α) for entire range (370–950 nm) utilizing the Aethalometer data and also provide the absorption coefficient (b_{abs}) and mass absorption efficiency (MAE: σ_{abs}) of these absorbing aerosols (BC and EC) for the study period from October 2008 to May 2009 in the IGP.

2. Materials and Methods

2.1. Site Description. The sampling site at Patiala (30.2°N; 76.3°E; 250 m above mean sea level) is located upwind of major population and industrial polluting sources in the Indo-Gangetic Plain (IGP; Figure 1). The site is strategically surrounded by agricultural fields (nearest distance ~1 km) and located in the state of Punjab, where over 84% of the land area is in use under the cultivation [12]. The present study has been carried out from October 2008 to May 2009. The entire study period from October to May is subdivided into three emission phases: October-November, referred to as postmonsoon, is influenced by emissions from postharvest paddy-residue burning; December–March, referred to as wintertime, is dominated by emissions from biofuel burning and fossil-fuel combustion [13]. Furthermore, the wintertime period in the IGP is associated with shallower atmospheric boundary layer and fog formation events. The time period from April to May, referred to as premonsoon, is influenced by postharvest wheat-residue burning emissions [13]. The period from June to September (SW-monsoon) is associated with frequent rain events that keep the ambient atmosphere relatively clean. For further details related to the site description, reference is made to our earlier publications [13, 14]. The important information on the assessment of emission budget of carbonaceous species (EC, OC, and polycyclic aromatic hydrocarbons) and determination of organic mass-to-organic carbon (OM/OC) ratio for these aerosol samples has been documented elsewhere [15, 16].

Figure 1: Map showing the sampling site at Patiala in the Indo-Gangetic Plain (IGP) in Northern India.

2.2. Methodology. The mass concentrations of BC from the sampling site at Patiala were determined by an Aethalometer (model: AE-31, Magee Scientific, USA). It monitors the optical attenuation (absorbance) of light at seven wavelengths (370, 470, 520, 590, 660, 880, and 950 nm) with a typical half-width of 20 nm [17]. However, the BC mass concentration is assessed at 880 nm wavelength. While determining the BC mass concentration using Aethalometer, the change in attenuation of light passing through the filter is monitored for a given interval of time. Assuming that BC is the only absorbing component in the atmospheric aerosols, a linear relationship of BC mass concentration with the change in attenuation of light is used to determine the BC mass concentration [8, 18]. In this study, the attenuation signal has been integrated for 5 minutes and flow rate was maintained at 3.4 L min^{-1}. The analytical uncertainty in BC measurements is ~±2% (as reported in the manual). However, it has also been reported that sometimes the BC mass concentrations can be overestimated due to presence of other absorbing aerosols in the atmosphere [19]. More details on the analytical technique of the Aethalometer can be found elsewhere [20, 21]. The Aethalometer uses a constant attenuation cross section (σ_{ATN}) of 16.6 m^2 g^{-1}, in determining the BC mass concentrations. The attenuation coefficient ($b_{ATN\text{-}AETH}$; Mm^{-1}) of BC from Aethalometer (at 880 nm) can be represented mathematically by the following equation:

$$b_{ATN\text{-}AETH} = \mathrm{BC}\left(\mu g/m^3\right) \times 16.6\left(m^2/g\right). \quad (1)$$

For the simultaneous determination of EC mass concentration from the same site, the ambient aerosols with

aerodynamic diameter less than 2.5 μm ($PM_{2.5}$) were collected onto the precombusted tissuquartz filters by filtering ambient air at a flow rate of ~1.2 $m^3\,min^{-1}$ using a high volume sampler (Thermo Scientific). During the first phase (October-November) of sampling, aerosols were collected for nearly 24 h continuously, whereas, during rest of the period, the sampling was integrated for 10–12 h for adequate aerosol collection. The EC mass concentrations were determined from a filter aliquot (1.5 cm^2 rectangular punch) using EC-OC analyzer (model 2000, Sunset Laboratory, USA), by NIOSH (National Institute for Occupational Safety and Health) thermooptical transmittance (TOT) protocol [22, 23]. Briefly, employing the thermooptical method on EC-OC analyzer, the organic carbon (OC) and elemental carbon (EC) are oxidized to CO_2 separately, by heating the aerosol sample in inert (helium) and oxidizing conditions (helium + oxygen), respectively. Subsequent conversion of CO_2 to methane (CH_4) by a methanator facilitates the quantification of OC and EC using a flame ionization detector (FID). The simultaneous monitoring of optical attenuation (ATN) from a laser source (at 678 nm) determines the split point between OC and EC and facilitates the correction for pyrolyzed carbon. Duplicate analysis of aerosols ($n = 45$) provided the uncertainty on OC and EC measurements to be within ±3% and ±7%, respectively [13]. Analytical accuracy in determining total carbon is assessed by analyzing known amount of potassium hydrogen phthalate (KHP) solution ($n = 16$); the average ratio of measured carbon to expected carbon is 1.05 ± 0.04 (Av ± sd). Analysis of several field-based samples ($n = 10$), spiked with sucrose, further ascertained the OC-EC split point and provides uncertainty on OC measurements of ±10% at most. The optical attenuation (ATN, a unitless parameter) of EC at 678 nm can be represented by the following equation:

$$\mathrm{ATN} = \ln\left(\frac{I_0}{I}\right). \tag{2}$$

The attenuation coefficient from EC-OC analyzer ($b_{\mathrm{ATN\text{-}ECOC}}$; Mm^{-1}) can be estimated from the ATN signal measured at 678 nm using the following equation:

$$b_{\mathrm{ATN\text{-}ECOC}}\left(\mathrm{Mm}^{-1}\right) = \mathrm{ATN} \times \left(\frac{A}{V}\right). \tag{3}$$

The terms A and V represent the aerosol loaded tissuquartz filter area ($400 \times 10^{-4}\,m^2$ for present study) and volume of air filtered for each sample collection (m^3), respectively. The attenuation cross section ($\sigma_{\mathrm{ATN\text{-}ECOC}}$, $m^2\,g^{-1}$) can be directly obtained by correcting the measured ATN signal for shadowing effect [R(ATN); explained later] and dividing by the EC concentration per unit area of the quartz filter (EC_S in $\mu g\,cm^{-2}$; surface loading of EC) as shown in the following equation:

$$\sigma_{\mathrm{ATN\text{-}ECOC}} = \left(\frac{\mathrm{ATN}}{R\,(\mathrm{ATN}) * \mathrm{EC_S}}\right). \tag{4}$$

The absorption coefficient of EC ($b_{\mathrm{abs\text{-}ECOC}}$, Mm^{-1}; $1M = 10^{-6}$) is calculated by the following equation:

$$b_{\mathrm{abs\text{-}ECOC}} = \left(\frac{A}{V} * \frac{\mathrm{ATN}}{R\,(\mathrm{ATN}) * C}\right), \tag{5}$$

where C and R(ATN) are the two empirical constants to correct the measured absorption signal for multiple scattering and shadowing effects, respectively. The value of $R = 1$ and $C = 2.827$ has been adopted as the correction factor for shadowing and multiple scattering effects for EC, respectively [24, 25].

Furthermore, the mass absorption efficiency of EC (MAE in $m^2\,g^{-1}$; $\sigma_{\mathrm{abs\text{-}ECOC}}$) is calculated by the following equation:

$$\mathrm{MAE} = \left(\frac{b_{\mathrm{abs}}}{\mathrm{EC}\left(\mu g\,m^{-3}\right)}\right). \tag{6}$$

It is important to state here that (5) and (6) are also applicable for BC, since filter substrate is of quartz fiber. For Aethalometer data, the values of $R = 1$ and $C = 2.355$, 2.656, 2.677, 2.733, 2.827, 2.933, and 2.925 have been used for seven wavelengths (370, 470, 520, 590, 660, 880, and 950 nm) [24, 25].

3. Results and Discussion

The temporal variability records in the mass concentrations of BC and EC and the BC-to-EC ratio are shown in Figures 2(a) and 2(b). The primary objective of this study is to assess the characteristics of elemental and black carbon (EC and BC) based on their mass absorption efficiency (MAE). This study has been conducted from an upwind site in the Indo-Gangetic Plain. The source characteristics of BC and EC are discussed below.

3.1. Aethalometer-Based BC. The average concentrations of BC are 15.4, 8.5, and 4.2 $\mu g\,m^{-3}$ during the paddy-residue burning emissions (October-November), bio- and fossil-fuel combustion, and wheat-residue burning emission, respectively. To assess the impact of different emission sources on Aethalometer-based BC at the measurement site, we have utilized a literature based approach [26, 27]. Basically, the method utilizes the percentage difference of BC mass concentrations measured at two different channels [i.e., $(BC_{370}–BC_{880})/BC_{880}$]. The positive ratio is indicator for the dominant contribution of biomass burning emissions [26]. Whereas, the negative ratio suggests for the dominant contribution of fossil-fuel combustion sources [27]. In our study, as evident from Figure 2(c), the $(BC_{370}–BC_{880})/BC_{880}$ ratio is positive for almost all the data points during the paddy-residue burning emission (October-November) and wheat-residue burning emission (April-May). During wintertime (December–March), this ratio varying between positive and negative indicates for the mixed contribution from fossil-fuel combustion sources and biomass burning emissions to BC mass concentration. A recent study has also estimated the percentage difference of BC mass concentration at two different stations during wintertime in India namely Delhi and Manora peak [28]. Their study reports positive ratio of

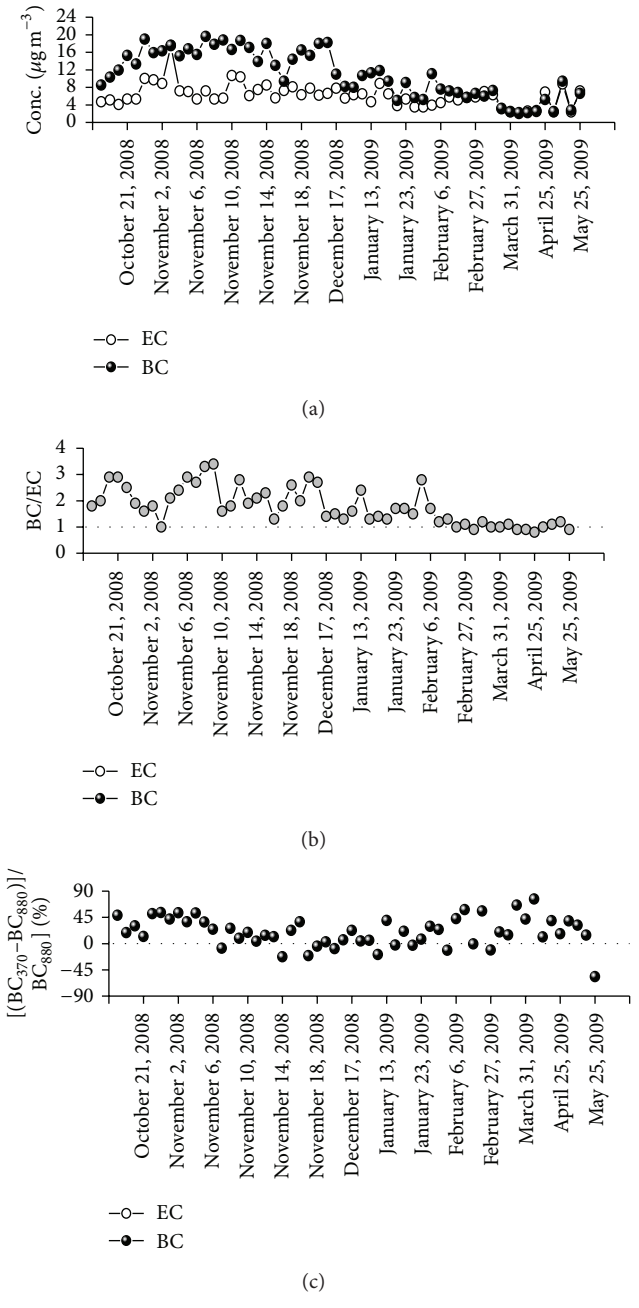

Figure 2: Temporal variability in the: (a) mass concentrations of BC and EC; (b) BC-to-EC ratio and; (c) percentage contribution of BC measured at 370 nm and 880 nm for different emissions during the study period from October 2008 to May 2009.

$(BC_{370}-BC_{880})/BC_{880}$ at both the stations during wintertime and attributes to dominant contribution of biomass burning emissions.

The variation of spectral absorption coefficient (b_{abs}) of BC during different emissions is shown in Figure 3. A power law is preferentially used to express the wavelength (λ) dependence of absorption coefficient (b_{abs}), as follows:

$$b_{abs} \propto \lambda^{-\alpha}. \quad (7)$$

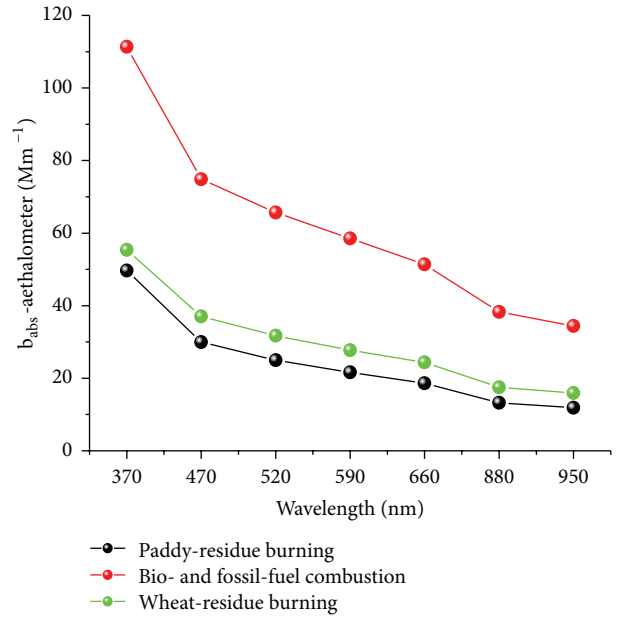

Figure 3: The spectral variation of averaged absorption coefficient (b_{abs}) of BC during different emissions in this study.

The Ångström exponent (α) is determined empirically using the Aethalometer based b_{abs} at multiwavelength (370–950 nm), from the power law (7), serving for comparison with other studies. In this study, the value of α is found to be 1.52 for paddy-residue burning emission, 1.25 for emissions from bio- and fossil-fuel combustion, and 1.32 from the wheat-residue burning emission in the Indo-Gangetic Plain. This information is hitherto unknown in the literature. In an earlier study [29], the authors report α value of 1.02 from a downwind location at Kanpur in the IGP. Another study distinguishes aerosol source based on differences in the wavelength dependence in light absorption [30]. The study reports for light absorption varying approximately as λ^{-1} (weak wavelength dependence) by the vehicular aerosols, indicating for BC to be the dominant absorbing component. In contrast, the aerosols from savanna biomass burning were found to have much stronger wavelength dependence, nearly λ^{-2} [30]. Literature based values suggest that α varies from 1 to 2.9 for BC derived from residential bio-fuel [31]. From our study in the Indo-Gangetic Plain, we document that light absorption by aerosol from postharvest agricultural-waste burning emissions exhibits wavelength dependence of approximately $\lambda^{-1.5}$.

3.2. EC-OC Analyzer Based EC. The organic carbon (OC) and non-sea-salt potassium (nss-K^+, a tracer of the biomass burning emission; Table 1) have been determined to assess diagnostic ratios of OC/EC and nss-K^+/EC in these emissions. The K^+ concentrations measured in aerosols using Ion-Chromatograph [23] have been corrected for the contribution from sea salts using the Na^+ tracer method and represented as nss-K^+ [32]. The $PM_{2.5}$ concentrations varied from 110 to 390 $\mu g\,m^{-3}$ during October-November during

Table 1: Ambient concentration and optical characteristics of black carbon (BC) and elemental carbon (EC) from different emissions in the Indo-Gangetic Plain (IGP).

Concentration ($\mu g\,m^{-3}$)	Paddy-residue burning (October-November; $n = 33$)	Bio- and fossil-fuel combustion (December–March; $n = 28$)	Wheat-residue burning (April-May; $n = 10$)
BC	8.5–19.6 (15.4 ± 3.0)	2.4–18.2 (8.5 ± 3.9)	2.2–9.4 (4.2 ± 2.7)
EC	3.8–17.5 (7.3 ± 2.7)	2.3–8.9 (5.3 ± 1.6)	2.0–8.8 (3.9 ± 2.6)
Characteristic ratios [range (Arithmetic average ± stdev)]			
OC/EC	4.6–25.7 (13.0 ± 4.6)	1.9–10.1 (5.6 ± 2.1)	2.5–6.5 (4.0 ± 1.1)
nss-K^+/EC	0.2–2.0 (0.8 ± 0.4)	0.1–0.8 (0.3 ± 0.2)	0.2–0.8 (0.4 ± 0.2)
BC/EC	1.0–3.4 (2.2 ± 0.6)	0.9–2.9 (1.6 ± 0.6)	0.8–1.2 (1.0 ± 0.1)
$b_{abs\text{-}AETH}$ (at 880 nm)	8–18 (13 ± 3)	7–64 (27 ± 17)	11–28 (16 ± 6)
$b_{abs\text{-}ECOC}$ (corrected for 880 nm)	8–55 (15 ± 9)	8–28 (15 ± 5)	7–20 (13 ± 5)
$b_{abs\text{-}AETH}/b_{abs\text{-}ECOC}$	0.3–1.6 (1.0 ± 0.3)	0.3–5.7 (2.0 ± 1.6)	1.0–1.5 (1.2 ± 0.2)

the postharvest paddy-residue burning emissions and 18 to 123 $\mu g\,m^{-3}$ during the wheat-residue burning emissions (April-May). The average concentration of OC is 92 $\mu g\,m^{-3}$ during the paddy-residue burning emission and 15 $\mu g\,m^{-3}$ during the wheat-residue burning emission. The $PM_{2.5}$ concentrations varied from 33 to 220 $\mu g\,m^{-3}$ and OC varied from 9 to 58 $\mu g\,m^{-3}$ during the bio- and fossil-fuel combustion period (December–March). The average concentrations of EC are 7.3, 5.3, and 3.9 $\mu g\,m^{-3}$ during October-November, December–March, and April-May, respectively (Table 1). The OC/EC ratio varied from 4.6 to 25.7 (Av: 13.0) during paddy-residue burning emission, 1.9 to 10.1 (Av: 5.6) during bio- and fossil-fuel combustion, and 2.5 to 6.5 (Av: 4.0) for the wheat-residue burning emission. The large temporal variability in the concentrations of particulate species and OC/EC ratio during the first (October-November: paddy-residue burning period) and third emission periods (April-May: wheat-residue burning) is attributable to the difference in the type of two biomass burning emissions and their source strength. Furthermore, the moisture contents in the two biomasses burned are also significantly different: moisture content of paddy-residue is 40–50% and wheat-residue is <5% [13]. However, during December–March, the variability in OC/EC ratio is attributable to varying contributions from bio-fuel burning emission and fossil-fuel combustion sources in the Indo-Gangetic Plain. Furthermore, the nss-K^+/EC ratio varied from 0.2 to 2.0 (Av: 0.8), 0.1 to 0.8 (Av: 0.3), and 0.2 to 0.8 (Av: 0.4) during these emissions. The K^+/EC ratios varying from ~0.1 to 0.6 have been reported earlier for characterization of different kinds of biomass burning emissions [33]. In this study, the nss-K^+/EC average ratio of ~0.4–0.8 is suggested to represent the biomass burning emissions in the Indo-Gangetic Plain.

3.3. Intercomparison of BC and EC. The mass concentrations of BC and EC varied from 2.2 to 19.6 $\mu g\,m^{-3}$ and from 2.0 to 17.5 $\mu g\,m^{-3}$, respectively, during the entire study period from October 2008 to May 2009. The mass concentrations of BC and EC exhibit near similar trends in seasonal variability with maximum during the paddy-residue burning and minimum during the wheat-residue burning emission. However, a significant difference in the concentrations of BC and EC measured by two different techniques was observed, in particular, during the paddy-residue burning emission (October-November). The difference between mass concentrations of BC and EC was relatively low (compared to paddy-residue burning) during wintertime (December–March), when emissions from bio-fuel burning and fossil-fuel combustion dominate in the Indo-Gangetic Plain (Table 1). Thus overall, during these two emission scenarios, the BC mass concentrations were always higher than the EC concentrations. In sharp contrast, the mass concentrations of BC and EC were quite similar during the wheat-residue burning period (April-May). The BC-to-EC ratio was 2.2 ± 0.6 during paddy-residue burning period, 1.6 ± 0.6 during emissions from bio-fuel burning and fossil-fuel combustion, and approach to unity (1.0 ± 0.1) during the wheat-residue burning period (Figure 2(b)). An earlier study [34] has suggested that the NIOSH type protocol operated at 850°C during the OC-EC split could lead to underestimation of EC up to ~25%. It is noteworthy to mention that even after correcting the measured concentration of EC by 25%, the BC-to-EC ratio becomes 1.8 ± 0.5, 1.2 ± 0.5, and 0.8 ± 0.1 during the aforementioned three consecutive emissions. Thus, the BC/EC ratios conspicuously greater than 1 in particular during paddy-residue burning emissions suggest assessing the contribution of light-absorbing organic aerosols in the IGP.

The scatter plots between BC/EC and OC/EC ratios are shown for different emissions in the IGP (Figures 4(a), 4(b), and 4(c)). During the paddy-residue burning emission (October-November), when OC/EC average ratio is 13.0 ± 4.6 [average OC: 92 $\mu g\,m^{-3}$; EC: 7.3 $\mu g\,m^{-3}$], the BC/EC average ratio is 2.2 ± 0.6 ($R = 0.49$; $P < 0.01$, Figure 4(a)). During wintertime (December–March), when emission from bio-fuel burning and fossil-fuel combustion is dominant source of carbonaceous aerosols in the IGP, the OC/EC average ratio is 5.6 ± 2.1 [average OC: 29 $\mu g\,m^{-3}$; EC: 5.3 $\mu g\,m^{-3}$] and the BC/EC average ratio is 1.6 ± 0.6 ($R = 0.90$; $P < 0.01$, Figure 4(b)). However, during the wheat-residue burning period (April-May; Figure 4(c)), when OC/EC average ratio is 4.0 ± 1.1 [average OC: 15 $\mu g\,m^{-3}$; EC: 3.9 $\mu g\,m^{-3}$], the BC/EC average ratio is 1.0 ± 0.1 (Table 1). Our investigations

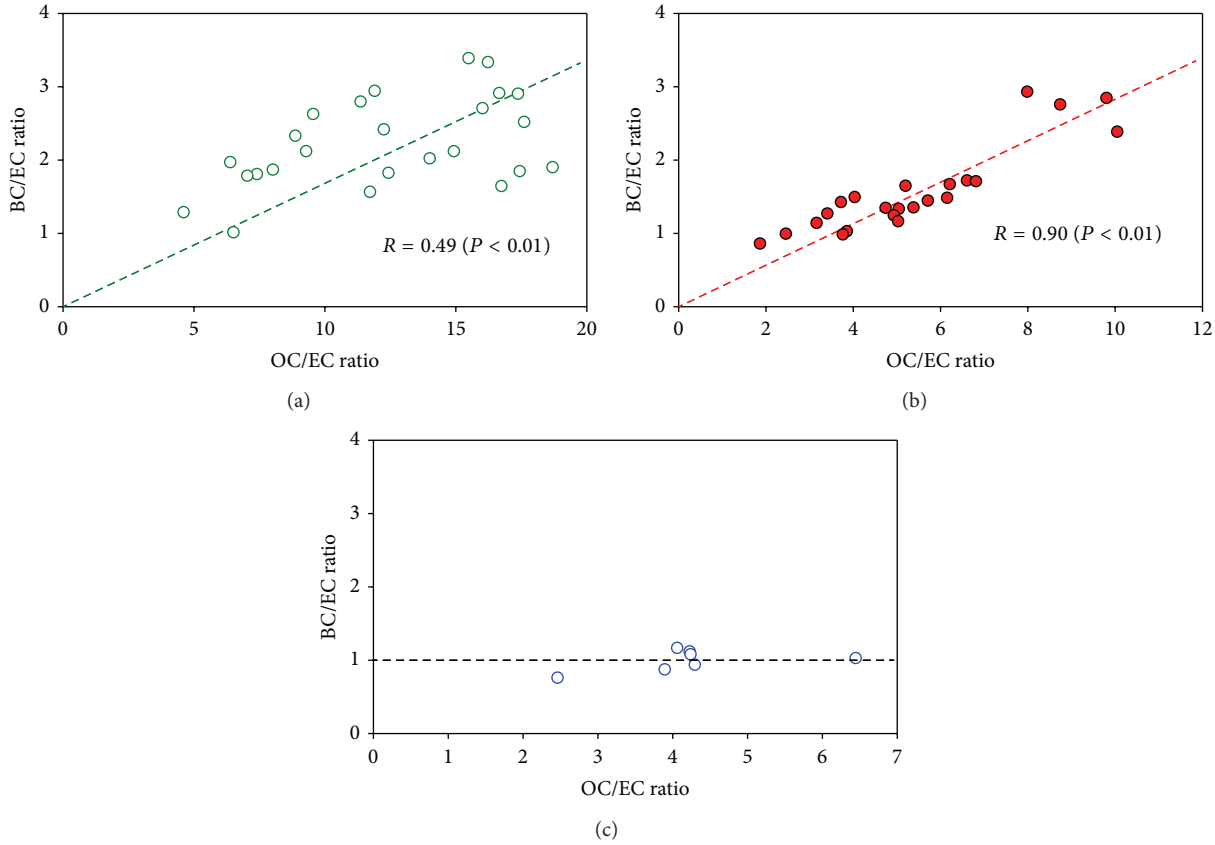

Figure 4: Scatter plots between the BC/EC ratio and OC/EC ratio during: (a) paddy-residue burning emission (October-November); (b) biofuel burning emission and fossil-fuel combustion (December–March); and (c) wheat-residue burning emission (April-May).

on comparing the mass concentrations of BC and EC during different emissions in the IGP suggest for relatively large difference between the two, by a factor of 2-3, when the mass concentrations of particulate OC, EC, and OC/EC ratios are relatively high (paddy-residue burning). In contrast, the Aethalometer-based BC and EC-OC analyzer based EC concentrations look quite similar when OC concentrations are less than 20 $\mu g\,m^{-3}$ and OC/EC ratio is ~2–4. In future, studies would be required to assess and address to the variability records of light-absorbing organic aerosol species from these large-scale biomass burning emissions in the IGP [2, 30].

The optical attenuation (ATN at 678 nm) from EC-OC analyzer is utilized to determine the attenuation cross section ($\sigma_{\text{ATN-ECOC}}$) during different emissions in the IGP. The scatter plot between the optical attenuation (ATN) and EC_s ($\mu g/cm^2$) during three different emissions exhibits a linear dependence with significant correlations ($R \geq 0.74$, $P < 0.01$; Figures 5(a), 5(b), and 5(c)). The slope of regression line for different emissions provides the attenuation cross section of EC. Accordingly, the attenuation cross section ($\sigma_{\text{ATN-ECOC}}$ at 678 nm) values are $7.2 \pm 0.4\,m^2\,g^{-1}$; $8.9 \pm 0.8\,m^2\,g^{-1,}$ and $9.1 \pm 0.7\,m^2\,g^{-1}$ for the paddy-residue burning emission (October-November), for emissions from bio-fuel burning and fossil-fuel combustion (December–March) and wheat-residue burning emission (April-May; Figures 5(a), 5(b), and 5(c)). After normalization at 880 nm the $\sigma_{\text{ATN-ECOC}}$ values are $4.8 \pm 0.3\,m^2\,g^{-1}$; $6.4 \pm 0.6\,m^2\,g^{-1}$;and $6.4 \pm 0.5\,m^2\,g^{-1}$ for the paddy-residue burning emission (October-November), for emissions from bio-fuel burning and fossil-fuel combustion (December–March) and wheat-residue burning emission (April-May), respectively. It is remarkable that all these values ($\sigma_{\text{ATN-ECOC}}$, at 880 nm) are ~30–40% of the attenuation cross section used in Aethalometer for the determination of BC mass concentration.

3.4. Absorption Coefficient and Mass Absorption Efficiency of EC and BC. Absorption coefficient of BC ($b_{\text{abs-AETH}}$) as well as EC ($b_{\text{abs-ECOC}}$) is the essential input parameters involved in the direct radiative forcing calculations. It is important to mention that the filter-based absorption technique yields systematic error in the optical attenuation (ATN) [9, 35]. In this context, suggestions from earlier studies to incorporate the corrections due to multiple scattering and shadowing effects have been applied [24, 25]. The $b_{\text{abs-AETH}}$ (at 880 nm) are ranging from 8–18 (13 ± 3) Mm^{-1}, 7–64 (27 ± 17) Mm^{-1}, and 11–28 (16 ± 6) Mm^{-1} during the paddy-residue burning emission, bio-fuel burning emission and fossil-fuel combustion, and wheat-residue burning emission, respectively (Table 1). The $b_{\text{abs-ECOC}}$ (at 678 nm) are ranging from 11–82 (22 ± 14) Mm^{-1}, 12–38 (21 ± 7) Mm^{-1}, and

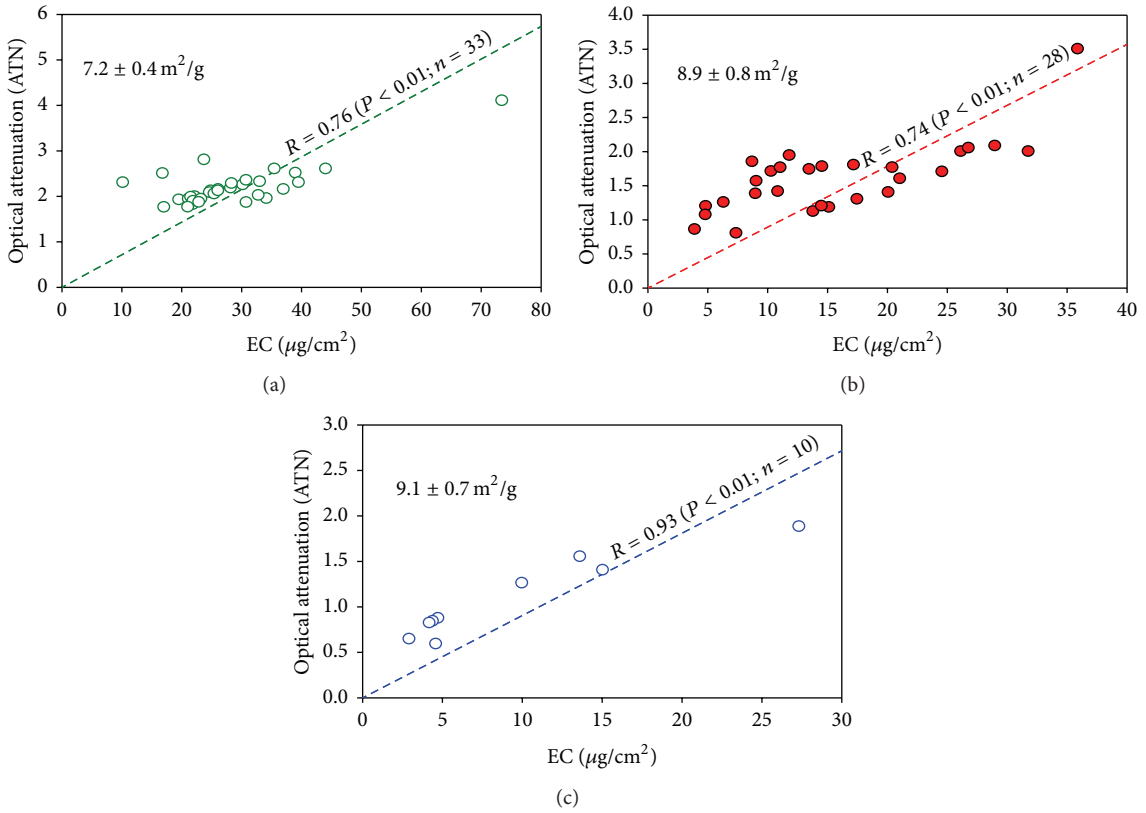

FIGURE 5: Attenuation cross section of EC at 678 nm ($\sigma_{\text{ATN-ECOC}}$ in $\text{m}^2\,\text{g}^{-1}$) during: (a) paddy-residue burning emission (October-November); (b) emissions from biofuel burning and fossil-fuel combustion (December–March); and (c) wheat-residue burning emission (April-May).

9–29 (18 ± 6) Mm^{-1} during the paddy-residue burning emission (October-November), bio-fuel burning emission and fossil-fuel combustion (December–March), and wheat-residue burning emission (April-May), respectively. Normalized to 880 nm, $b_{\text{abs-ECOC}}$ (at 880 nm) are ranging from 8–55 (15 ± 9) Mm^{-1}, 8–28 (15 ± 5) Mm^{-1}, and 7–20 (13 ± 5) Mm^{-1} during the paddy-residue burning emission, bio-fuel burning emission and fossil-fuel combustion, and wheat-residue burning emission, respectively. Relatively high values of $b_{\text{abs-ECOC}}$ (as high as 55 Mm^{-1}) during the paddy-residue burning emission (during October-November) indicate the high light absorption characteristics of EC in the ambient air during this period as compared to those during the other emissions, assessed in this study (wheat-residue burning during April-May and bio- and fossil-fuel combustion during December–March). The average ratio of $b_{\text{abs-AETH}}/b_{\text{abs-ECOC}}$ (at 880 nm) for the postharvest paddy- and wheat-residue burning emissions is close to 1. In sharp contrast, this ratio is ~2 for emissions from bio- and fossil-fuel combustion in the IGP. The Aethalometer based mass absorption efficiency (MAE) of BC (at 880 nm) is 0.9 ± 0.1 $\text{m}^2\,\text{g}^{-1}$, 3.5 ± 2.2 $\text{m}^2\,\text{g}^{-1}$, and 4.4 ± 1.3 $\text{m}^2\,\text{g}^{-1}$ during paddy-residue burning emission, bio-fuel burning emission and fossil-fuel combustion, and wheat-residue burning emission. The MAE (at 678 nm) of EC has been determined by the linear regression analysis between absorption coefficients (b_{abs}; Mm^{-1}) and EC mass concentration ($\mu\text{g}\,\text{m}^{-3}$). The slope of regression line gives the MAE for different emissions impacting the sampling site. Accordingly, the MAE of EC (at 678 nm) are 3.0 ± 0.8 $\text{m}^2\,\text{g}^{-1}$ ($R = 0.57$, $P < 0.01$), 3.8 ± 0.8 $\text{m}^2\,\text{g}^{-1}$ ($R = 0.78$, $P < 0.01$), and 4.1 ± 0.4 $\text{m}^2\,\text{g}^{-1}$ ($R = 0.93$, $P < 0.01$) during paddy-residue burning emission (October-November), bio-fuel burning emission and fossil-fuel combustion (December–March), and wheat-residue burning emission (April-May). Normalizing to 880 nm, the MAE of EC (at 880 nm) are 2.0 ± 0.5 $\text{m}^2\,\text{g}^{-1}$ ($R = 0.57$, $P < 0.01$), 2.7 ± 0.6 $\text{m}^2\,\text{g}^{-1}$ ($R = 0.78$, $P < 0.01$), and 2.9 ± 0.3 $\text{m}^2\,\text{g}^{-1}$ ($R = 0.93$, $P < 0.01$) during paddy-residue burning emission, bio-fuel burning emission and fossil-fuel combustion, and wheat-residue burning emission (Figure 6). The literature based values on MAE of EC suggest for a wide range, varying from 2 to 25 $\text{m}^2\,\text{g}^{-1}$, depending on its emission source and mixing state of EC [9, 18, 36, 37]. For example, [18] has reported a value of 7.5 ± 1.2 $\text{m}^2\,\text{g}^{-1}$ (at 550 nm), for the uncoated soot particles. Furthermore, the freshly emitted particles coexist as external mixture of light scattering and absorbing (EC) components [38, 39]. Subsequently, during the course of transport away from its emission source, these aerosols undergo internal mixing. Towards this, the global simulation models suggest that in ~1–5 days, the EC can be internally mixed with other aerosols [3]. After mixing, the physicochemical characteristics of pure EC will no longer be retained, due to the coating of other aerosols such as sulfate

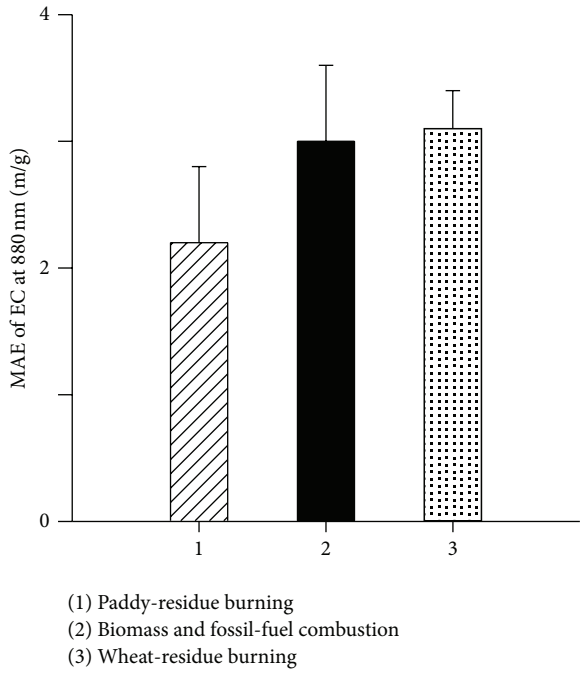

FIGURE 6: Mass absorption efficiency (MAE; $m^2\,g^{-1}$) of EC at 880 nm during different emissions in Northern India.

and organics. The MAE of coated-EC has been reported to be relatively high as compared to that for the uncoated EC [40]. The plausible mechanism for enhancement in the MAE of EC due to coating is widely referred to as the lensing effect, focusing the light into core of EC. In this study, we report the MAE of EC (at 880 nm) from two distinct postharvest biomass burning emissions (paddy-residue burning: $2.0 \pm 0.5\,m^2\,g^{-1}$; wheat-residue burning: $2.9 \pm 0.3\,m^2\,g^{-1}$) and during the emissions from bio- and fossil-fuel combustion (MAE: $2.7 \pm 0.6\,m^2\,g^{-1}$; December–March). A near similar MAE of EC varying from 3.0 to $6.8\,m^2\,g^{-1}$ at 632 nm from biomass burning emissions had also been reported earlier [41]. In contrast, the MAE from diesel exhaust has been found relatively high (Av: $8.4\,m^2\,g^{-1}$) [41]. Thus, the MAE of EC centering at $2.7\,m^2\,g^{-1}$ during December–March period suggests that biomass burning emission is the dominant source of EC. However, future studies are needed in order to assess the impact of mixing state on the MAE of BC and EC in the Indo-Gangetic Plain.

4. Summary

This study has been carried out from October 2008 to May 2009 at Patiala, an upwind location in the Indo-Gangetic Plain (Northern India). The important conclusions drawn from this study are as follows.

(1) The OC/EC ratio varying from 4.6 to 25.7 (Av ± sd: 13.0 ± 4.6) and nss-K^+/EC ratio varying from 0.2 to 2.0 (0.8 ± 0.4) have been recorded from the postharvest paddy-residue burning emission (October-November). In contrast, during the postharvest wheat-residue burning emission during April-May, the OC/EC ratio varied from 2.5 to 6.5 (Av ± sd: 4.0 ± 1.1) and nss-K^+/EC ratio varied from 0.2 to 0.8 (0.4 ± 0.2). Furthermore, the inference on dominance of biomass burning emissions during the period from December to March has been made, using the nss-K^+/EC ratio (chemical tracer) of 0.3±0.2 (range: 0.1–0.8) in conjunction with the OC/EC ratio of 5.6 ± 2.1 (range: 1.9–10.1).

(2) Overall, the BC mass concentrations varied from 2 to 20 $\mu g\,m^{-3}$, and the EC concentrations varied from 2 to 18 $\mu g\,m^{-3}$. The BC/EC ratios are significantly higher (2.2 ± 0.6) during the postharvest paddy-residue burning emission (October-November), decrease to 1.6 ± 0.6 during emissions from bio-fuel burning and fossil-fuel combustion (December–March) and 1.0 ± 0.1 during the wheat-residue burning emission (April-May).

(3) The BC/EC ratios conspicuously greater than 1 have been observed during paddy-residue burning emission (October-November), associated with high abundance of EC, OC, and OC/EC ratio. This suggests assessing the contribution of light-absorbing organic aerosol species.

(4) The light absorption by aerosol from postharvest agricultural-waste (paddy- and wheat-residue) burning emissions exhibits wavelength dependence of approximately $\lambda^{-1.5}$.

(5) The attenuation cross section ($\sigma_{ATN\text{-}ECOC}$) inferred from EC-OC analyzer at 880 nm is ~30–40% lower than that used in the Aethalometer.

(6) The mass absorption efficiency (MAE; σ_{abs}) of EC at 880 nm is $2.0 \pm 0.6\,m^2\,g^{-1}$, $2.7 \pm 0.6\,m^2\,g^{-1}$, and $2.9 \pm 0.3\,m^2\,g^{-1}$ during paddy-residue burning, emissions from bio-fuel burning and fossil-fuel combustion, and wheat-residue burning emission, respectively.

Conflict of Interests

The authors declare that there is no conflict of interests regarding the publication of this paper.

Acknowledgments

This work is financially supported by ISRO-Geosphere Biosphere Program (Bengaluru, India). The authors thank the anonymous reviewers for their constructive comments and suggestions and Dr. Lucas Alados-Arboledas for the Editorial handling of this paper.

References

[1] A. Petzold, J. A. Ogren, M. Fiebig et al., "Recommendations for the interpretation of "black carbon" measurements," *Atmospheric Chemistry and Physics*, vol. 13, pp. 8365–8379, 2013.

[2] M. O. Andreae and A. Gelencsér, "Black carbon or brown carbon? The nature of light-absorbing carbonaceous aerosols,"

Atmospheric Chemistry and Physics, vol. 6, no. 10, pp. 3131–3148, 2006.

[3] M. Z. Jacobson, "Strong radiative heating due to the mixing state of black carbon in atmospheric aerosols," *Nature*, vol. 409, no. 6821, pp. 695–697, 2001.

[4] S. Solomon, D. Qin, M. Manning et al., Eds., *Climate Change 2007: The Physical Science Basis. Contribution of Working Group I to the Fourth Assessment Report of the Intergovernmental Panel on Climate Change*, Cambridge University Press, Cambridge, UK, 2007.

[5] C. Wang, D. Kim, A. M. L. Ekman, M. C. Barth, and P. J. Rasch, "Impact of anthropogenic aerosols on Indian summer monsoon," *Geophysical Research Letters*, vol. 36, no. 21, Article ID L21704, 2009.

[6] W. K. M. Lau, M.-K. Kim, K.-M. Kim, and W.-S. Lee, "Enhanced surface warming and accelerated snow melt in the Himalayas and Tibetan Plateau induced by absorbing aerosols," *Environmental Research Letters*, vol. 5, no. 2, Article ID 025204, pp. 1–10, 2010.

[7] M. V. Ramana, V. Ramanathan, Y. Feng et al., "Warming influenced by the ratio of black carbon to sulphate and the black-carbon source," *Nature Geoscience*, vol. 3, no. 8, pp. 542–545, 2010.

[8] D. C. Snyder and J. J. Schauer, "An inter-comparison of two black carbon aerosol instruments and a semi-continuous elemental carbon instrument in the urban environment," *Aerosol Science and Technology*, vol. 41, no. 5, pp. 463–474, 2007.

[9] C. Liousse, H. Cachier, and S. G. Jennings, "Optical and thermal measurements of black carbon aerosol content in different environments: variation of the specific attenuation cross-section, sigma (σ)," *Atmospheric Environment A*, vol. 27, no. 8, pp. 1203–1211, 1993.

[10] K. Ram, M. M. Sarin, and S. N. Tripathi, "Inter-comparison of thermal and optical methods for determination of atmospheric black carbon and attenuation coefficient from an urban location in northern India," *Atmospheric Research*, vol. 97, no. 3, pp. 335–342, 2010.

[11] K. Ram and M. M. Sarin, "Absorption coefficient and site-specific mass absorption efficiency of elemental carbon in aerosols over urban, rural, and high-altitude sites in India," *Environmental Science and Technology*, vol. 43, no. 21, pp. 8233–8239, 2009.

[12] K. V. S. Badarinath, T. R. K. Chand, and V. K. Prasad, "Agriculture crop residue burning in the Indo-Gangetic Plains—a study using IRS-P6 AWiFS satellite data," *Current Science*, vol. 91, no. 8, pp. 1085–1089, 2006.

[13] P. Rajput, M. M. Sarin, R. Rengarajan, and D. Singh, "Atmospheric polycyclic aromatic hydrocarbons (PAHs) from post-harvest biomass burning emissions in the Indo-Gangetic Plain: isomer ratios and temporal trends," *Atmospheric Environment*, vol. 45, no. 37, pp. 6732–6740, 2011.

[14] D. Sharma, D. Singh, and D. Sumit, "Case studies of black carbon aerosol characteristics during agriculture crop residue burning period over Patiala, Punjab, India using the synergy of ground based and satellite observations," *International Journal of Geology, Earth and Environmental Sciences*, vol. 2, no. 2, pp. 315–326, 2012.

[15] P. Rajput, M. M. Sarin, D. Sharma, and D. Singh, "Characteristics and emission budget of carbonaceous species from post-harvest agricultural-waste burning in source region of the Indo-Gangetic Plain," *Tellus B*, vol. 66, Article ID 21026, 2014.

[16] P. Rajput and M. M. Sarin, "Polar and non-polar organic aerosols from large-scale agricultural-waste burning emissions in Northern India: implications to organic mass-to-organic carbon ratio," *Chemosphere*, 2013.

[17] A. D. A. Hansen, *The Aethalometer Manual*, Magee Scientific, Berkeley, Calif, USA, 2005.

[18] T. C. Bond and R. W. Bergstrom, "Light absorption by carbonaceous particles: an investigative review," *Aerosol Science and Technology*, vol. 40, no. 1, pp. 27–67, 2006.

[19] A. D. A. Hansen, V. N. Kapustin, V. M. Kopeikin, D. A. Gillette, and B. A. Bodhaine, "Optical absorption by aerosol black carbon and dust in a desert region of Central Asia," *Atmospheric Environment A*, vol. 27, no. 16, pp. 2527–2531, 1993.

[20] A. D. A. Hansen, H. Rosen, and T. Novakov, "The aethalometer—an instrument for the real-time measurement of optical absorption by aerosol particles," *Science of the Total Environment*, vol. 36, pp. 191–196, 1984.

[21] A. D. A. Hansen, *Magee Scientific Aethalometer User's Guide*, Magee Scientific, Berkeley, Calif, USA, 1996.

[22] M. E. Birch and R. A. Cary, "Elemental carbon-based method for monitoring occupational exposures to particulate diesel exhaust," *Aerosol Science and Technology*, vol. 25, no. 3, pp. 221–241, 1996.

[23] R. Rengarajan, M. M. Sarin, and A. K. Sudheer, "Carbonaceous and inorganic species in atmospheric aerosols during wintertime over urban and high-altitude sites in North India," *Journal of Geophysical Research: Atmospheres*, vol. 112, no. D21, Article ID D21307, 2007.

[24] P. R. Sinha, R. K. Manchanda, D. G. Kaskaoutis, Y. B. Kumar, and S. Sreenivasan, "Seasonal variation of surface and vertical profile of aerosol properties over a tropical urban station Hyderabad, India," *Journal of Geophysical Research: Atmospheres*, vol. 118, no. 2, pp. 749–768, 2013.

[25] O. Schmid, P. Artaxo, W. P. Arnott et al., "Spectral light absorption by ambient aerosols influenced by biomass burning in the Amazon Basin. I: comparison and field calibration of absorption measurement techniques," *Atmospheric Chemistry and Physics*, vol. 6, no. 11, pp. 3443–3462, 2006.

[26] M. Wang, S. Ghan, M. Ovchinnikov et al., "Aerosol indirect effects in a multi-scale aerosol-climate model PNNL-MMF," *Atmospheric Chemistry and Physics*, vol. 11, no. 11, pp. 5431–5455, 2011.

[27] H. Herich, C. Hueglin, and B. Buchmann, "A 2.5 year's source apportionment study of black carbon from wood burning and fossil fuel combustion at urban and rural sites in Switzerland," *Atmospheric Measurement Techniques*, vol. 4, no. 7, pp. 1409–1420, 2011.

[28] A. K. Srivastava, K. Ram, P. Pant, P. Hegde, and H. Joshi, "Black carbon aerosols over Manora Peak in the Indian Himalayan foothills: implications for climate forcing," *Environmental Research Letters*, vol. 7, no. 1, Article ID 014002, 2012.

[29] S. Dey and S. N. Tripathi, "Estimation of aerosol optical properties and radiative effects in the Ganga basin, northern India, during the wintertime," *Journal of Geophysical Research: Atmospheres*, vol. 112, no. D3, Article ID D03203, 2007.

[30] T. W. Kirchstetter, T. Novakov, and P. V. Hobbs, "Evidence that the spectral dependence of light absorption by aerosols is affected by organic carbon," *Journal of Geophysical Research: Atmospheres*, vol. 109, no. D21, Article ID D21208, 2004.

[31] T. C. Bond, "Spectral dependence of visible light absorption by carbonaceous particles emitted from coal combustion,"

Geophysical Research Letters, vol. 28, no. 21, pp. 4075–4078, 2001.

[32] W. C. Keene, A. A. P. Pszenny, J. N. Galloway, and M. E. Hawley, "Sea-salt corrections and interpretation of constituent ratios in marine precipitation," *Journal of Geophysical Research: Atmospheres*, vol. 91, no. D6, pp. 6647–6658, 1986.

[33] M. O. Andreae and P. Merlet, "Emission of trace gases and aerosols from biomass burning," *Global Biogeochemical Cycles*, vol. 15, no. 4, pp. 955–966, 2001.

[34] F. Cavalli, M. Viana, K. E. Yttri, J. Genberg, and J.-P. Putaud, "Toward a standardised thermal-optical protocol for measuring atmospheric organic and elemental carbon: the EUSAAR protocol," *Atmospheric Measurement Techniques*, vol. 3, no. 1, pp. 79–89, 2010.

[35] A. Petzold, C. Kopp, and R. Niessner, "The dependence of the specific attenuation cross-section on black carbon mass fraction and particle size," *Atmospheric Environment*, vol. 31, no. 5, pp. 661–672, 1997.

[36] S. Sharma, J. R. Brook, H. Cachier, J. Chow, A. Gaudenzi, and G. Lu, "Light absorption and thermal measurements of black carbon in different regions of Canada," *Journal of Geophysical Research: Atmospheres*, vol. 107, no. D24, p. 4771, 2002.

[37] J. P. Schwarz, R. S. Gao, J. R. Spackman et al., "Measurement of the mixing state, mass, and optical size of individual black carbon particles in urban and biomass burning emissions," *Geophysical Research Letters*, vol. 35, no. 13, Article ID L13810, 2008.

[38] M. Pósfai, R. Simonics, J. Li, P. V. Hobbs, and P. R. Buseck, "Individual aerosol particles from biomass burning in southern Africa: 1. Compositions and size distributions of carbonaceous particles," *Journal of Geophysical Research: Atmospheres*, vol. 108, no. D13, pp. 1–19, 2003.

[39] M. Mallet, J. C. Roger, S. Despiau, P. Putaud, and O. Dubovik, "A study of the mixing state of black carbon in urban zone," *Journal of Geophysical Research: Atmospheres*, vol. 109, no. D4, Article ID D04202, 2004.

[40] R. W. Bergstrom, T. P. Ackerman, and L. W. Richards, "The optical properties of particulate elemental carbon," in *Particulate Carbon: Atmospheric Life Cycle*, G. T. Wolff and R. L. Klimsch, Eds., Plenum Press, New York, NY, USA, 1982.

[41] Y. Cheng, K.-B. He, M. Zheng et al., "Mass absorption efficiency of elemental carbon and water-soluble organic carbon in Beijing, China," *Atmospheric Chemistry and Physics*, vol. 11, no. 22, pp. 11497–11510, 2011.